

RESEARCH ARTICLE | DECEMBER 01 2025

Coherence enhanced by detrained oscillators: Breaking π -reflection symmetry FREE

Hyunsuk Hong  ; Jae Sung Lee  ; Hyunggyu Park  

 Check for updates

Chaos 35, 121101 (2025)

<https://doi.org/10.1063/5.0304615>



View
Online



Export
Citation

Articles You May Be Interested In

Two-scale structure of the current layer controlled by meandering motion during steady-state collisionless driven reconnection

Phys. Plasmas (July 2004)

Single particle motion near an X point and separatrix

Phys. Plasmas (June 2004)

Coherence enhanced by detrained oscillators: Breaking π -reflection symmetry

Cite as: Chaos 35, 121101 (2025); doi: 10.1063/5.0304615

Submitted: 29 September 2025 · Accepted: 10 November 2025 ·

Published Online: 1 December 2025



Hyunsuk Hong,¹ Jae Sung Lee,² and Hyunggyu Park^{3,a}

AFFILIATIONS

¹Department of Physics and Research Institute of Physics and Chemistry, Jeonbuk National University, Jeonju 54896, South Korea

²School of Physics, Korea Institute for Advanced Study, Seoul 02455, South Korea

³Quantum Universe Center, Korea Institute for Advanced Study, Seoul 02455, South Korea

^aAuthor to whom correspondence should be addressed: hgpark@kias.re.kr

ABSTRACT

We study a generalized Kuramoto model in which each oscillator carries two coupled phase variables, representing a minimal swarming system. Assuming perfect correlation between the intrinsic frequencies associated with each phase variable, we identify a novel dynamic mode characterized by bounded oscillatory motion that breaks the π -reflection symmetry. This symmetry breaking enhances global coherence and gives rise to a non-trivial mixed state, marked by distinct degrees of ordering in each variable. Numerical simulations confirm our analytic predictions for the full phase diagram, including the nature of the transition. Our results reveal a fundamental mechanism through which detrained (dynamic) oscillators can promote global synchronization, offering broad insights into coupled dynamical systems beyond the classical Kuramoto paradigm.

Published under an exclusive license by AIP Publishing. <https://doi.org/10.1063/5.0304615>

Collective synchronization is a hallmark of many complex systems, ranging from flashing fireflies and applauding audiences to neuronal networks and power grids. The Kuramoto model has long served as a fundamental theoretical framework for understanding how simple oscillators achieve synchronization through mutual interactions. In this work, we extend this classical paradigm by considering oscillators that possess two coupled phase variables, providing a minimal mathematical description of the so-called swarming systems—entities that both move and synchronize. We uncover a previously unreported dynamical regime in which oscillators exhibit bounded oscillations, leading to spontaneous breaking of the π -reflection symmetry of detrained oscillators. This broken symmetry enhances global coherence and gives rise to an interesting mixed state where the two phase variables display distinct degrees of order. This mechanism provides new insight into how coupled internal and external degrees of freedom shape collective dynamics, with potential relevance to biological swarms, active matter, and coupled electronic oscillators.

I. INTRODUCTION

The study of coupled oscillators has long been central to understanding collective behavior in complex dynamical systems,^{1–8} with real-world applications ranging from biological rhythms^{9–14} to synchronization in social networks.^{15–17} The Kuramoto model¹⁸ and its variants have provided deep insights into how global coherence can emerge against intrinsic disorder.^{18–22} Recently, more attention has been paid to systems that exhibit both synchronization and spatial self-organization, such as “swarming systems.”²³ A minimal extension of the Kuramoto model for such systems considers oscillators with two coupled variables; an internal phase and a secondary (often spatial) variable, both evolving on a periodic domain. Interactions between these variables lead to mutual reinforcement between spatial aggregation and phase synchronization, giving rise to a variety of long-term collective states. These include synchronized clusters, phase waves, and mixed states characterized by strong ordering in one variable and weak ordering in the other.^{24–26} However, the mechanisms underlying such states, particularly the emergence of mixed states, remain poorly understood. In this work, we explore a

simplified yet physically insightful limit of the swarmalator model, in which the intrinsic frequencies associated with the two phase variables are perfectly correlated. This assumption retains essential features of the coupling while allowing an analytically tractable framework.

Our most notable finding is the identification of a new dynamical mode; oscillators that are not phase-locked to a fixed point but instead exhibit bounded oscillations with zero mean velocity. Crucially, these oscillators contribute to collective orderings through interphase coupling. Using a perturbative approach, we quantify their impact on the order parameters and show that their dynamics break the π -reflection symmetry in the phase distribution. This symmetry breaking results in a nonzero contribution from detrained (dynamic) oscillators to the order parameter—a feature absent in the standard Kuramoto model.³ Our findings provide deeper insight into general coupled oscillator systems including swarmalator systems, by highlighting the critical roles of coupling asymmetry, frequency correlations, and dynamic entrainment in shaping collective behavior.

II. MODEL

We consider a system of N Kuramoto oscillators with two phase variables. The dynamics of these variables are governed by the coupled differential equations

$$\dot{x}_i = v_i + \frac{J}{N} \sum_{j=1}^N \sin(x_j - x_i) \cos(\theta_j - \theta_i), \quad (1)$$

$$\dot{\theta}_i = \omega_i + \frac{K}{N} \sum_{j=1}^N \sin(\theta_j - \theta_i) \cos(x_j - x_i), \quad (2)$$

where x_i and θ_i are the phase variables of oscillator i ($i = 1, \dots, N$), each with period 2π , accompanied by intrinsic frequencies v_i and ω_i drawn randomly from given distributions. Each variable evolves according to the Kuramoto-type dynamics, but with a coupling strength modulated by the difference in the other variable. This cross-modulated interaction promotes a mutual enhancement of local synchrony of both phases for sufficiently large and positive J and K .

By interpreting x_i as the position of the i th oscillator, Eqs. (1) and (2) effectively describe the dynamics of mobile oscillators with the internal phase θ_i on a one-dimensional (1D) ring with length 2π . Phase synchrony in the x_i variables corresponds to spatial aggregation (swarming) of oscillators, which is enhanced by synchrony in the internal phases. Conversely, the tendency toward phase synchronization is amplified by spatial clustering of oscillators. These mechanisms capture the hallmark behavior of swarmalator systems, i.e., the co-emergence of spatial structure and phase coherence.

This model, initially studied in Refs. 24 and 25 and later with thermal noise replacing quenched intrinsic frequencies,²⁶ exhibits several long-term states, including incoherent, phase wave, synchronized, and mixed states. In this paper, we go beyond the identification of these states to investigate the underlying mechanisms that govern the behavior of both entrained (static) and detrained

(dynamic) oscillators, as well as their distinct roles in shaping the collective dynamics of the system.

The model studied in this work is primarily mathematical in nature. Nevertheless, it can serve as a minimal representation of certain real systems, such as the population of calling frogs or Janus particles navigating pseudo-one-dimensional grooves or channels. Although this study presents a toy model for such systems, it offers a useful framework for reproducing and elucidating various intriguing phenomena observed in real-world settings.²⁴

III. CORRELATED INTRINSIC FREQUENCIES

In previous studies, the intrinsic frequencies v_i and ω_i were drawn independently, implying no correlation between them. Although some degree of correlation may exist in real-world systems, such correlations are generally expected to have limited influence on the system's collective behavior, except for transition thresholds and potentially critical scalings. Here, we explore the extreme case of perfect correlation by setting $v_i = \omega_i$ for all i . This simplifying assumption not only allows for more tractable analytical treatments but also provides insight into the behavior of the original, more general model. For mathematical convenience, we assume the intrinsic frequencies follow a symmetric Lorenzian distribution, $g(\omega) = \frac{\gamma}{\pi} \frac{1}{\omega^2 + \gamma^2}$, centered at zero with width γ .

The global ordering typically measured by the standard Kuramoto order parameter³ fails to capture the collective behavior in this model.^{24–26} Instead, a more suitable order parameter is the correlation between x_i and θ_i , which effectively characterizes the collective states. This observation naturally motivates a reformulation of the dynamic equations in terms of new variables that explicitly encode the correlations between position and phase. In this context, by introducing the variables $X_i = x_i + \theta_i$ and $Y_i = x_i - \theta_i$, Eqs. (1) and (2) can be rewritten as

$$\dot{X}_i = 2\omega_i + J_+ S_+ \sin(\Phi_+ - X_i) + J_- S_- \sin(\Phi_- - Y_i), \quad (3)$$

$$\dot{Y}_i = J_- S_+ \sin(\Phi_+ - X_i) + J_+ S_- \sin(\Phi_- - Y_i), \quad (4)$$

where $J_{\pm} = \frac{J \pm K}{2}$ and S_{\pm} are the magnitudes of the complex order parameters Z_{\pm} , defined as

$$Z_{\pm} \equiv S_{\pm} e^{i\Phi_{\pm}} = \frac{1}{N} \sum_{j=1}^N e^{iX_j} (Y_j). \quad (5)$$

Here, $S_{\pm} (\geq 0)$ quantify the degree of coherence in the X and Y variables, respectively, while Φ_{\pm} denote the corresponding mean phases. By assuming that S_{\pm} and Φ_{\pm} approach time-independent constants in the long-time limit, as expected for the symmetric $g(\omega)$, we may, without loss of generality, set $\Phi_{\pm} = 0$.

As in the original model,²⁵ we expect various long-term collective states to emerge: (a) An incoherent (disordered) state with $(S_+, S_-) = (0, 0)$, (b) a phase wave state with $(0, S)$ or $(S, 0)$, (c) a mixed state with (S_1, S_2) , where $S_1 \neq S_2$ and both are finite, and (d) a synchronized (ordered) state with (S, S) . Due to the introduction of the correlation between v_i and ω_i , the symmetry between the X and Y variables is explicitly broken.²⁷ As a consequence, the internal symmetry between S_+ and S_- , which was present in the original

model, is no longer preserved. In fact, the synchronized state with (S, S) is not realizable except in special limiting cases. On the other hand, the absence of intrinsic frequency in the Y dynamics (a consequence of the perfect correlation) renders the mathematical analysis of the system significantly more tractable.

When $J_- = 0$ (i.e., $J = K$), the dynamics of X and Y become decoupled, as seen in Eqs. (3) and (4). The X variable follows the standard Kuramoto dynamics with intrinsic frequency 2ω and coupling strength J_+ . As is well known,³ the oscillators are divided into two distinct groups in the long-time limit; entrained (static) oscillators, which settle into fixed points with $\dot{X}_i = 0$ and detrained (dynamic) oscillators, which circulate incessantly with a nonzero mean velocity. It is noteworthy that only the static oscillators contribute to the order parameter S_+ . In contrast, the Y variable, having zero intrinsic frequency, evolves according to the Watanabe-Strogatz (WS) dynamics.²⁸ In this case, for any $J_+ > 0$, all oscillators become static and thus contribute fully to the order parameter S_- . The long-time behavior of the order parameters is then given as follows: $(S_+, S_-) = (0, 0)$ for $J_+ < 0$ (incoherent), $(0, 1)$ for $0 < J_+ < 4\gamma$ (phase wave), and $(S, 1)$ with $S = \sqrt{1 - 4\gamma/J_+}$ for $J_+ > 4\gamma$ (mixed). Thus, the system exhibits a discontinuous jump in S_- from 0 to 1 at $J_+ = 0$, and a continuous transition in S_+ at $J_+ = 4\gamma$.

When $J_- \neq 0$ (i.e., $J \neq K$), on the other hand, the dynamics of X and Y are coupled, leading to a nontrivial interplay between the orderings in the X and Y variables. We note that the system retains a symmetry under the transformation of $J_- \rightarrow -J_-$ and, therefore, restrict our analysis to the case of $J_- \geq 0$, from now on, without loss of generality.

Let us first consider the $S_+ = 0$ solution. In this case, the Y dynamics is unaffected by X , even when $J_- \neq 0$, resulting in $S_- = 1$ with $Y_i = \Phi_-$ for $J_+ > 0$, and $S_- = 0$ for $J_+ < 0$. The X dynamics then simplifies to $\dot{X}_i = 2\omega_i$, leading to $S_+ = 0$ for all values of J_+ , thus ensuring the self-consistency of the solution. As usual, the $(0, 1)$ solution for $J_+ > 0$ is expected to lose stability against solutions with nonzero S_+ as J_+ increases further beyond a certain threshold. In that regime, the Y dynamics becomes influenced by the X variable through the emergence of nonzero S_+ [see Eq. (4)], which in turn reduces the Y ordering ($S_- < 1$). This reduction feeds back into the X dynamics, further altering S_+ , and the cycle continues. This mutual feedback eventually settles into a new steady state characterized by $S_+ > 0$ and $S_- < 1$. As J_- increases, the coupling between X and Y strengthens, further disrupting the ordering in X . Accordingly, the onset of nonzero S_+ is delayed compared to the $J_- = 0$ case. This overall qualitative picture is consistent with the phase diagram shown in Fig. 1, which will be analytically derived and numerically confirmed later.

Most interestingly, for finite S_+ , the Y variable may exhibit a new type of dynamic behavior, neither static (i.e., fixed point) nor fully dynamic with nonzero mean velocity. For small S_+ , the solution of Eq. (4) would involve a weak periodic modulation in time, induced by the X dynamics, around the mean phase angle Φ_- [see Eqs. (S36), (S46), and (S50) in the [supplementary material](#)]. This time-dependent modulation persists even in the long-time limit, particularly for oscillators with sufficiently large ω_i , where X_i continues to evolve with a finite mean velocity. These oscillators are not static in the usual sense with respect to the Y variable, since

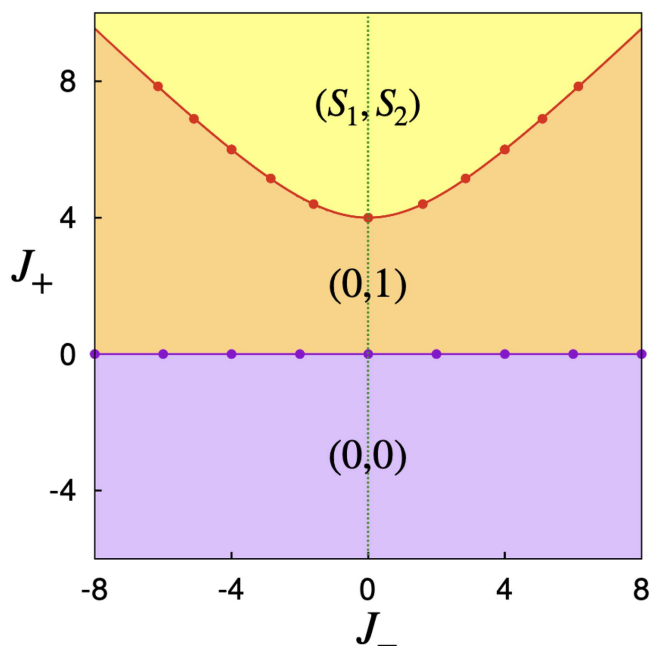


FIG. 1. Phase diagram in the (J_-, J_+) plane for $\gamma = 1$. Purple and red circles represent numerical results from simulations, while solid lines indicate theoretical predictions. The red curve corresponds to the hyperbolic transition line given by Eq. (13).

they do not converge to a fixed point, but their mean phase velocity vanishes, as Y_i does not circulate but instead undergoes bounded oscillations around Φ_- . This type of bounded dynamic motion leads to a reduction in the Y ordering ($S_- < 1$). However, the effect on the X ordering is more subtle and nontrivial, as it feeds back through the coupling and alters the collective dynamics in a more intricate manner.

IV. ANALYTIC RESULTS

To investigate the influence of this new dynamic mode on the order parameters, we employ a perturbation approach, treating S_+ as a small parameter near the transition. As a first step, we decompose the contributions to the order parameters into two components, arising from static and dynamic oscillators, respectively. For convenience, the newly identified dynamical mode, characterized by bounded oscillations, is included in the dynamic contribution. This decomposition is expressed as

$$S_{\pm} = S_{\pm}^s + S_{\pm}^d = \frac{1}{N} \sum_{j \in \Lambda_s} e^{iX_j(Y_j)} + \frac{1}{N} \sum_{j \in \Lambda_d} e^{iX_j(Y_j)}, \quad (6)$$

where Λ_s and Λ_d denote the sets of static and dynamic oscillators, respectively. Static oscillators, characterized by a stable fixed point ($\dot{X}_i = 0$ and $\dot{Y}_i = 0$), are described by

$$X_i = \sin^{-1} \left(\frac{\omega_i}{aS_+} \right), \quad \text{and} \quad Y_i = -\sin^{-1} \left(\frac{\omega_i}{bS_-} \right), \quad (7)$$

with $a = \frac{J_-^2 - J_+^2}{2J_+}$ and $b = \frac{J_+^2 - J_-^2}{2J_-}$, and the \sin^{-1} function is restricted to the first quadrant $[0, \pi/2]$. This fixed-point solution exists only when both conditions, $|\omega_i/a| \leq S_+$ and $|\omega_i/b| \leq S_-$, are satisfied. Moreover, a stability analysis requires $a, b > 0$, i.e., $J_+ > J_-$ (supplementary material). Since we expect $aS_+ \leq bS_-$ in the small S_+ regime (with $S_- \lesssim 1$), the constraint for the existence of fixed point solutions simplifies to $|\omega_i| \leq aS_+$. In the limit $N \rightarrow \infty$, the static contribution to the X ordering is given by²⁹

$$\begin{aligned} S_+^s &= \int_{-aS_+}^{aS_+} e^{i \sin^{-1}[\omega/(aS_+)]} g(\omega) d\omega \\ &= \frac{\gamma}{aS_+} \left[\sqrt{1 + \left(\frac{aS_+}{\gamma} \right)^2} - 1 \right] \\ &= \frac{1}{2} \left(\frac{aS_+}{\gamma} \right) - \frac{1}{8} \left(\frac{aS_+}{\gamma} \right)^3 + \mathcal{O}(S_+^5), \end{aligned} \quad (8)$$

where we used $g(\omega) = \frac{\gamma}{\pi} \frac{1}{\omega^2 + \gamma^2}$. As expected, the imaginary part vanishes. A similar expression for S_-^s can be derived as $S_-^s = \frac{2}{\pi} \left(\frac{aS_+}{\gamma} \right) + \mathcal{O}(S_+^3)$ [see Eq. (S93) in the supplementary material].

To calculate the contribution from dynamic oscillators, S_+^d , we consider the average probability distribution $P_\omega^d(X)$ for a given intrinsic frequency ω in the long-time limit. This leads to the following expression:

$$S_+^d = \int_{|\omega| > aS_+} d\omega g(\omega) \int_{-\pi}^{\pi} dX e^{iX} P_\omega^d(X). \quad (9)$$

Deriving the exact form of $P_\omega^d(X)$ is generally intractable. However, in the small- S_+ limit, a perturbative expansion becomes possible. In this regime, S_- remains close to unity, so we set $S_+ = \varepsilon$ with $\varepsilon \ll 1$ and approximate $S_- \approx 1 - d_1 \varepsilon - d_2 \varepsilon^2$, with constants d_1 and d_2 to be determined. Expanding all relevant terms up to $\mathcal{O}(\varepsilon^2)$, we derive an analytical expression for $P_\omega^d(X)$, which is rather complicated (see the supplementary material for the explicit expression).

A key feature of $P_\omega^d(X)$, arising from the coupling with the Y variable, is the breaking of the π -reflection symmetry,

$$P_\omega^d(X) \neq P_\omega^d(\pi - X), \quad (10)$$

indicating that $P_\omega^d(X)$ is not purely a function of $\sin(X)$, but also contains $\cos(X)$ -like components [see Eqs. (S59) and (S52) in the supplementary material]. These cosine-like terms originate from the influence of the new dynamic mode of Y variables, mediated by the coupling term when $J_- \neq 0$. In contrast, this symmetry is preserved in the standard Kuramoto model resulting in a vanishing real part of the dynamic contribution to the order parameter in Eq. (9); $\int_{-\pi}^{\pi} dX \cos(X) P_\omega^d(X) = 0$. In our case, however, the symmetry breaking leads to a nonzero real contribution to the order parameter. This symmetry breaking is primarily exhibited by slightly detrained oscillators (see the supplementary material). The numerical evidence of the π -reflection symmetry breaking

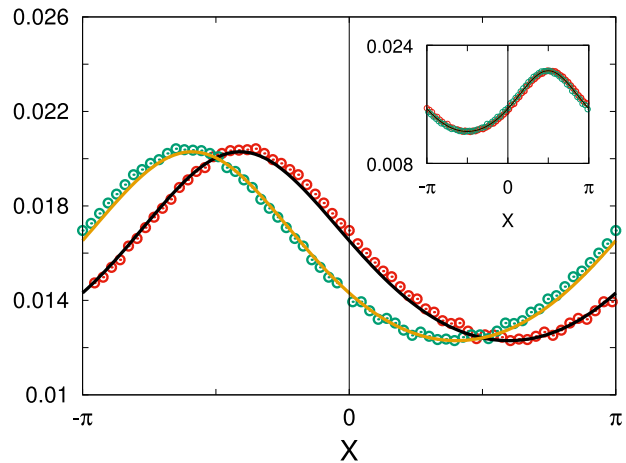


FIG. 2. The π -reflection symmetry breaking of the average probability distribution function $P_\omega^d(X)$ for a detrained (dynamic) oscillator. The data (red open circles) are obtained from numerical simulations with $N = 819, 200$, using the parameters $J = 9$, $K = 3$, and $\omega = 4.37$ ($> aS_+$), showing excellent agreement with the theoretical prediction (black solid line) given by Eq. (S59) in the supplementary material. For comparison, the same data are replotted with respect to $\pi - X$ (green open circles and orange line), clearly demonstrating the breaking of the π -reflection symmetry: $P_\omega^d(X) \neq P_\omega^d(\pi - X)$. The inset shows the corresponding results for $J = K = 5$ ($J_- = 0$), where the π -reflection symmetry is preserved.

[Eq. (10)] is presented in Fig. 2 for a typical detrained (dynamic) oscillator with $\omega > aS_+$.

After a lengthy calculation (supplementary material), we obtain

$$S_+^d \approx c_1 S_+ - c_2 S_+^2, \quad (11)$$

with non-negative coefficients given by $c_1 = \frac{J_-^2}{2J_+ (J_+ + 2\gamma)}$ and $c_2 = \frac{4aJ_-^2}{3\pi\gamma J_+^2}$. This result clearly demonstrates that *the ordering is enhanced by dynamic oscillators*, at least within the small- S_+ regime. Combining the contributions from both static and dynamic oscillators, we arrive at the following self-consistent equation as

$$S_+ = \left(\frac{a}{2\gamma} + c_1 \right) S_+ - c_2 S_+^2 + \mathcal{O}(S_+^3). \quad (12)$$

This equation always admits the trivial solution $S_+ = 0$ and a nontrivial solution emerges when the linear coefficient satisfies $\frac{a}{2\gamma} + c_1 - 1 > 0$. The nontrivial solution is always stable against the trivial one, so the transition from the $(0, 1)$ (phase wave) to the (S_1, S_2) (mixed) state occurs at the critical line given by $\frac{a}{2\gamma} + c_1 - 1 = 0$, which yields the following hyperbolic transition line in the (J_-, J_+) plane as

$$(J_+ - \gamma)^2 - J_-^2 = (3\gamma)^2. \quad (13)$$

For comparison, in the absence of dynamic contributions (i.e., setting $c_1 = 0$), the corresponding transition line is given by $(J_+ - 2\gamma)^2 - J_-^2 = (2\gamma)^2$. Since the actual transition line always

lies below this reference curve, we conclude that the presence of dynamic oscillators enhances the ordering in X , resulting in an *earlier onset of synchronization*. It is noteworthy that the self-consistent equation includes a quadratic term S_+^2 , which is absent in the standard Kuramoto model. As a result, the order parameter S_+ grows linearly near the transition point, characterized by the order parameter exponent $\beta_+ = 1$, in contrast to the Kuramoto model where $\beta = 1/2$.

The order parameter S_- , associated with the Y variable, can be evaluated in a similar manner (supplementary material) and is given by

$$S_- = S_-^s + S_-^d = 1 - \frac{c_1}{2} S_+^2 + \mathcal{O}(S_+^3), \quad (14)$$

where the linear terms from static and dynamic contributions cancel out exactly. As S_- begins to deviate from 1 (perfect ordering) due to the onset of a nonzero S_+ , the corresponding transition occurs along the same transition line given by Eq. (13). The reduction in S_- is proportional to S_+^2 , corresponding to $d_1 = 0$ and $d_2 = \frac{c_1}{2}$, which implies a quadratic decay near the transition with the exponent $\beta_- = 2$.

We note that the nature of the transition depends on the characteristics of the frequency distribution $g(\omega)$, as in the conventional Kuramoto model. As long as the distribution is symmetric and

unimodal, such as the Gaussian or Lorentzian forms considered in this study, the transition nature is expected to be universal.

V. NUMERICAL SIMULATIONS

We perform numerical simulations to support the analytic results. The self-consistent equations, Eqs. (3) and (4), are integrated iteratively, using the order parameters defined by Eq. (5). The system is initialized with random phase values, and time integration is carried out using Heun's method³⁰ for $M_t = 10^5$ time steps with a discrete interval $dt = 0.01$. To ensure the system reaches a steady state, the first half of the simulation ($M_t/2$) is discarded, and the order parameters S_\pm are computed by averaging over the remaining time steps. The total number of oscillators is set to $N = 10^5$, and we use $\gamma = 1$.

Figure 3 shows the behavior of S_\pm as a function of J_+ for a fixed value of $J_- = 4$. The analytic results predict an abrupt transition from the $(0, 0)$ state to the $(0, 1)$ state at $J_+ = 0$, followed by a continuous transition to the (S_1, S_2) state at $J_+ = \gamma + \sqrt{J_-^2 + (3\gamma)^2} = 6$ [see Eq. (13)]. These predictions are in excellent agreement with numerical results. Furthermore, the critical behaviors of the order parameters, characterized by the exponents $\beta_+ = 1$ and $\beta_- = 2$, are also confirmed numerically (see Fig. S2 in the supplementary material). Importantly, neglecting the contribution from dynamic oscillators leads to incorrect threshold and exponent values [see Eq. (S30) in the supplementary material], as indicated by the purple line in Fig. 3. In the special case $J_- = 0$, dynamic contributions vanish and the purple line agrees with numerical data, yielding the expected exponent $\beta_+ = 1/2$, as illustrated in the inset of Fig. 3.

VI. CONCLUSION

We investigated a population of Kuramoto oscillators with two coupled phase variables, representing a minimal model for more general swarmalator systems. By assuming a perfect correlation between the intrinsic frequencies associated with each phase variable, we obtain a simplified yet analytically tractable version of the model that retains essential physical features.

A central result of our study is the identification of a novel dynamic mode characterized by bounded oscillations, which induces π -reflection symmetry breaking in the dynamics of the coupled phase. This symmetry breaking draws dynamic oscillators into contributing positively to global ordering, thereby enhancing overall coherence and lowering the coherence threshold. As a result, the mixed state emerges prior to the onset of the symmetric synchronized state.

This form of π -reflection symmetry breaking is reminiscent of the transition from apolar nematic to polar symmetry in systems composed of non-spherical objects, such as liquid crystals,³¹ active matter,³² and various biological systems. Our findings suggest that this type of symmetry breaking through inter-variable coupling may serve as a general mechanism for an earlier onset of ordering in a broad class of coupled dynamical systems. Consistent with this view, preliminary studies of the original uncorrelated model also reveal spontaneous π -reflection symmetry breaking and the earlier emergence of coherence in the form of mixed states, preceding the symmetric synchronized state.

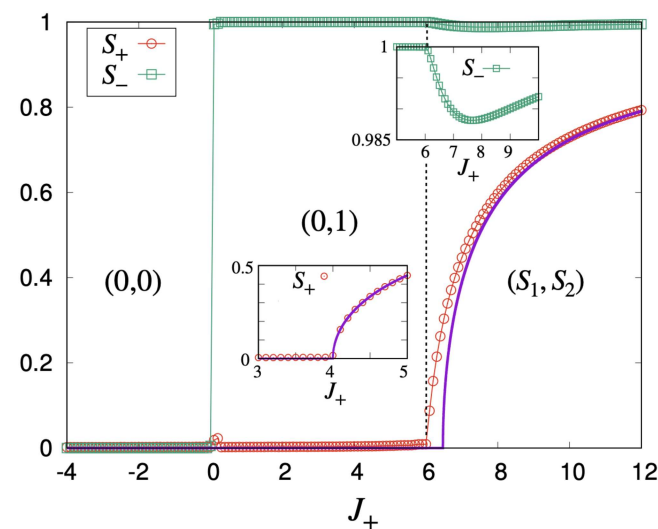


FIG. 3. The order parameters S_\pm are plotted as functions of J_+ for $J_- = 4$ and $\gamma = 1$. Open red circles and green squares represent numerical data for S_+ and S_- , respectively, in excellent agreement with analytical predictions, including transition points and their nature. The order parameter S_- exhibits a discontinuous jump from 0 to 1 at $J_+ = 0$ and remains nearly constant at 1 thereafter, except for a slight dip beginning around $J_+ = 6$ (see upper inset). At this point, S_+ begins to grow continuously. Both S_+ and S_- approach 1 asymptotically as $J_+ \rightarrow \infty$, without crossing. The solid purple line corresponds to the prediction obtained by neglecting dynamic contributions, which clearly deviates from the numerical data. For comparison, the lower inset shows the results for the case with $J_- = 0$. Vertical lines indicate the boundaries between different regimes: $(0, 0)$, $(0, 1)$, and (S_1, S_2) .

SUPPLEMENTARY MATERIAL

See the [supplementary material](#) for additional derivations and figures supporting this work.

ACKNOWLEDGMENTS

We thank J. Um for useful discussions at the early stage of this work. This research was supported by the National Research Foundation of Korea (NRF) grant funded by the Korea Government (MSIT) [Grant Nos. RS-2024-00348768) (H.H.) and 2017R1D1A1B06035497 (H.P.)] and individual KIAS [Grant Nos. PG064902 (J.S.L.) and QP013602 (H.P.)] at the Korea Institute for Advanced Study.

AUTHOR DECLARATIONS

Conflict of Interest

The authors have no conflicts to disclose.

Author Contributions

Hyunsuk Hong: Conceptualization (equal); Data curation (lead); Formal analysis (equal); Investigation (equal); Methodology (equal); Software (lead); Validation (equal); Visualization (equal); Writing – original draft (lead); Writing – review & editing (equal). **Jae Sung Lee:** Conceptualization (equal); Formal analysis (equal); Investigation (equal); Methodology (equal); Validation (equal); Visualization (equal); Writing – original draft (equal); Writing – review & editing (equal). **Hyunggyu Park:** Conceptualization (equal); Formal analysis (equal); Investigation (equal); Methodology (equal); Validation (equal); Visualization (equal); Writing – original draft (equal); Writing – review & editing (equal).

DATA AVAILABILITY

The data that support the findings of this article are not publicly available upon publication because it is not technically feasible and/or the cost of preparing, depositing, and hosting the data would be prohibitive within the terms of this research project. The data that support the findings of this study are available from the corresponding author upon reasonable request.

REFERENCES

- 1 A. T. Winfree, *The Geometry of Biological Time* (Springer, 2001).
- 2 J. D. Crawford, *J. Stat. Phys.* **74**, 1047 (1994); J. D. Crawford, *Phys. Rev. Lett.* **74**, 4341 (1995); J. D. Crawford and K. T. R. Davies, *Physica D* **125**, 1 (1999).
- 3 Y. Kuramoto, in *International Symposium on Mathematical Problems in Theoretical Physics*, edited by H. Araki, Springer Lecture Notes Physics Vol. 39 (Springer, New York, 1975), p. 420; *Chemical Oscillations, Waves, and Turbulence* (Springer, Berlin, 1984); Y. Kuramoto and I. Nishikawa, *J. Stat. Phys.* **49**, 569 (1987).
- 4 S. H. Strogatz and R. E. Mirollo, *J. Stat. Phys.* **63**, 613 (1991); S. H. Strogatz, R. E. Mirollo, and P. C. Matthews, *Phys. Rev. Lett.* **68**, 2730 (1992); M. K. S. Yeung and S. H. Strogatz, *Physica D* **143**, 1 (2000).
- 5 S. H. Strogatz, *Sync: The Emerging Science of Spontaneous Order* (Hyperion, New York, 2003).
- 6 A. Pikovsky, M. Rosenblum, and J. Kurths, *Synchronization: A Universal Concept in Nonlinear Sciences* (Cambridge University Press, Cambridge, 2003).
- 7 H. Daido, *Prog. Theor. Phys.* **88**, 1213 (1992); H. Daido, *Phys. Rev. Lett.* **73**, 760 (1994).
- 8 J. A. Acebron, L. L. Bonilla, C. J. P. Vicente, F. Ritort, and R. Spigler, *Rev. Mod. Phys.* **77**, 137 (2005).
- 9 J. Buck and E. Buck, *Science* **159**, 1319 (1968).
- 10 C. S. Peskin, *Mathematical Aspects of Heart Physiology* (Courant Institute of Mathematical Sciences, New York, 1975), p. 268.
- 11 C. M. Gray, P. König, A. K. Engel, and W. Singer, *Nature* **338**, 334 (1989).
- 12 C. Liu, D. R. Weaver, S. H. Strogatz, and S. M. Reppert, *Cell* **91**, 855 (1997); S. H. Strogatz, R. E. Kronauer, and C. A. Czeisler, *Am. J. Physiol.* **253**, R172–R178 (1987).
- 13 J. J. Hopfield and A. V. Herz, *Proc. Natl. Acad. Sci. U.S.A.* **92**, 6655 (1995).
- 14 C. Kirst, T. Geisel, and M. Timme, *Phys. Rev. Lett.* **102**, 068101 (2009).
- 15 E. Ott and T. M. Antonsen, *Chaos* **27**, 051101 (2017).
- 16 A. Arenas, A. Díaz-Guilera, J. Kurths, Y. Moreno, and C. Zhou, *Phys. Rep.* **469**, 93 (2008).
- 17 Z. Néda, E. Ravasz, T. Vicsek, Y. Brechet, and A. L. Barabási, *Phys. Rev. E* **61**, 6987 (2000).
- 18 H. Daido, *Phys. Rev. Lett.* **68**, 1073 (1992); J. C. Stiller and G. Radons, *Phys. Rev. E* **58**, 1789 (1998); H. Daido, *Phys. Rev. Lett.* **61**, 2145 (2000); J. C. Stiller and G. Radons, *Phys. Rev. Lett.* **61**, 2148 (2000); B. Ottino-Löffler and S. H. Strogatz, *Phys. Rev. Lett.* **120**, 264102 (2018).
- 19 E. A. Martens, E. Barreto, S. H. Strogatz, E. Ott, P. So, and T. M. Antonsen, *Phys. Rev. E* **79**, 026204 (2009).
- 20 H. Hong and S. H. Strogatz, *Phys. Rev. Lett.* **106**, 054102 (2011); H. Hong and S. H. Strogatz, *Phys. Rev. E* **84**, 046202 (2011); *ibid.* **85**, 056210 (2012).
- 21 H. Hong, H. Park, and M. Y. Choi, *Phys. Rev. E* **72**, 036217 (2005); H. Hong, H. Chaté, H. Park, and L.-H. Tang, *Phys. Rev. Lett.* **99**, 184101 (2007).
- 22 H. Sakaguchi, S. Shinomoto, and Y. Kuramoto, *Prog. Theor. Phys.* **79**, 600 (1988); S.-W. Son and H. Hong, *Phys. Rev. E* **81**, 061125 (2010); I. V. Tyulkina, D. S. Golodbin, L. S. Klimenko, and A. Pikovsky, *Phys. Rev. Lett.* **120**, 264101 (2018).
- 23 K. P. O’Keeffe, H. Hong, S. H. Strogatz, and F. Wuest, *Nat. Commun.* **8**, 1 (2017).
- 24 K. P. O’Keeffe, S. Ceron, and K. Petersen, *Phys. Rev. E* **105**, 014211 (2022); Z. G. Nicolaou, D. Eroglu, and A. E. Motter, *Phys. Rev. X* **9**, 011017 (2019).
- 25 S. Yoon, K. P. O’Keeffe, J. F. F. Mendes, and A. V. Goltsev, *Phys. Rev. Lett.* **129**, 208002 (2022).
- 26 H. Hong, K. P. O’Keeffe, J. S. Lee, and H. Park, *Phys. Rev. Res.* **5**, 023105 (2023).
- 27 Introducing correlations between ω_i and v_i generates distinct frequency distributions (or distribution widths) for the transformed variables, X_i and Y_i . In the case of perfect correlation, the corresponding distribution width associated with the Y variable vanishes, leading to zero intrinsic frequency for all oscillators [see Eq. (4)].
- 28 S. Watanabe and S. H. Strogatz, *Phys. Rev. Lett.* **70**, 2391 (1993); S. Watanabe and S. H. Strogatz, *Physica D* **74**, 197 (1994); J. Um, H. Hong, and H. Park, *Sci. Rep.* **14**, 6816 (2024).
- 29 See [supplementary material](#) for additional derivations and figures.
- 30 See, e.g., R.L. Burden and J.D. Faires, *Numerical Analysis* (Brooks/Cole, Pacific Grove, 1997), p. 280.
- 31 D. Andrienko, *J. Mol. Liq.* **267**, 520 (2018).
- 32 V. Venkatesh, N. de Graaf Sousa, and A. Doostmohammadi, *J. Phys. A: Math. Theor.* **58**, 263001 (2025).